(10) Montfort, J. P.; Marin, G.; Monge, Ph. *Macromolecules* **1986**, *19*, 393, 1979.
(11) Graessley, W. W.; Struglinski, M. J. *Macromolecules* **1986**, *19*, 1754.
(12) Prest, W. M.; Porter, R. S. *J. Polym. Sci., Polym. Phys. Ed.* **1972**, *10*, 1639.
(13) Chuang, H. K.; Han, C. D. *J. Appl. Polym. Sci.* **1984**, *29*, 2205.
(14) Aoki, Y. *Polym. J. (Tokyo)* **1984**, *16*, 431.
(15) Han, C. D.; Yang, H. H. *J. Appl. Polym. Sci.* **1987**, *33*, 1199.
(16) Martuscelli, E.; Vicini, L.; Sever, A. *Makromol. Chem.* **1987**, *188*, 607.
(17) Krause, S. In *Polymer Blends*; Paul, D. R., Newman, S., Eds.; Academic Press: New York, 1978; Chapter 2.
(18) Olabisi, O.; Robeson, L. M.; Shaw, M. T. *Polymer-Polymer Miscibility*; Academic Press: New York, 1979; Chapter 5.
(19) Weeks, N. E.; Karasz, F. E.; MacKnight, W. J. *J. Appl. Phys.* **1977**, *48*, 4068.
(20) Fried, J. R.; Karasz, F. E.; MacKnight, W. J. *Macromolecules* **1978**, *11*, 150.
(21) Wignall, C. D.; Child, H. R.; Li-Aravena, F. *Polymer* **1980**, *17*, 640.
(22) Kambour, R. P.; Bopp, R. C.; Maconnachie, A.; MacKnight, W. J. *Polymer* **1980**, *21*, 133.
(23) Stejskal, E. O.; Schaefer, J.; Sefcik, M. D.; McKay, R. A. *Macromolecules* **1981**, *14*, 276.
(24) Additional data at 190 and 200 °C have been taken, after the publication of ref 13 in 1984.
(25) Wu, S. *J. Polym. Sci., Part B: Polym. Phys.* **1987**, *25*, 557.
(26) Noland, J. S.; Hsu, H. H. C.; Saxon, R.; Schmitt, J. M. In *Multicomponent Polymer Systems*; Platzer, N. A. J., Ed.; Advances in Chemistry 99; American Chemical Society: Washington, DC, 1971; p 99.
(27) Paul, D. R.; Altamirano, J. O. In *Copolymers, Polyblends and Composites*; Platzer, N. A. J., Ed.; Advances in Chemistry 142; American Chemical Society: Washington, DC, 1975; p 371.
(28) Nishi, T.; Wang, T. T. *Macromolecules* **1975**, *8*, 909.
(29) Kwei, T. K.; Frisch, H. L.; Radigan, W.; Vogel, S. *Macromolecules* **1977**, *10*, 157.
(30) Wang, T. T.; Nishi, T. *Macromolecules* **1977**, *10*, 142.
(31) This has been possible because, while presenting master curves of the dynamic storage modulus $G'(\omega)$ and dynamic loss modulus $G''(\omega)$ versus ωa_T, Aoki reported the numerical values of the parameters that were used to calculate values of a temperature shift factor a_T.
(32) Hall, W. J.; Kruse, R. L.; Mendelson, R. A.; Trementozzi, Q. A. *Org. Coat. Appl. Polym. Sci. Proc.* **1982**, *47*, 298.
(33) Paul, D. R.; Barlow, J. W. *Polymer* **1984**, *25*, 487.
(34) Shiomo, T.; Karasz, F. E.; MacKnight, W. J. *Macromolecules* **1986**, *19*, 2274.
(35) McMaster, L. P. *Macromolecules* **1973**, *6*, 760.
(36) Seefried, C. G.; Koleske, J. V. *J. Test. Eval.* **1976**, *4*, 220.
(37) Koleske, J. V. In *Polymer Blends*; Paul, D. R., Newman, S., Eds.; Academic Press: New York, 1978; Chapter 22.
(38) Chiu, S. C.; Smith, T. G. *J. Appl. Polym. Sci.* **1984**, *29*, 1781, 1797.
(39) Han, C. D.; Yang, H. H., unpublished research, 1986.
(40) Wu, S. *Polymer* **1987**, *28*, 1144.
(41) Stein, D. J.; Jung, R. H.; Illers, K. H.; Hendus, H. *Angew. Makromol. Chem.* **1974**, *36*, 89.
(42) McMaster, L. P. In *Copolymer, Polyblends and Composites*; Platzer, N. A., Ed.; Advances in Chemistry 142, American Chemical Society, Washington, DC, 1975; p 43.
(43) Kruse, W. A.; Kirste, R. G.; Haas, J.; Schmitt, B. J.; Stein, D. J. *Makromol. Chem.* **1976**, *177*, 1145.
(44) Bernstein, R. E.; Cruz, C. A.; Paul, D. R.; Barlow, J. W. *Macromolecules* **1977**, *10*, 681.
(45) Naito, K.; Johnson, E. E.; Allara, K. L.; Kwei, T. K. *Macromolecules* **1978**, *11*, 1260.
(46) McBrierty, V. J.; Douglass, D. C.; Kwei, T. K. *Macromolecules* **1978**, *11*, 1265.
(47) Doi, M.; Edwards, S. F. *J. Chem. Soc., Faraday Trans. 2* **1978**, *74*, 1789, 1802, 1818.
(48) Graessley, W. W. *Adv. Polym. Sci.* **1982**, *47*, 67.
(49) Han, C. D.; Yang, H. H., unpublished research, 1987.
(50) Wendorff, J. H. *J. Polym. Sci., Polym. Lett. Ed.* **1980**, *18*, 439.
(51) Schmitt, B. J.; Kirste, R. G.; Jelenic, J. *Makromol. Chem.* **1980**, *181*, 1655.
(52) Han, C. D.; Lem, K. W. *Polym. Eng. Rev.* **1983**, *2*, 135.
(53) Han, C. D.; Chuang, H. K. *J. Appl. Polym. Sci.* **1985**, *30*, 2431.
(54) Han, C. D.; Ma, Y. J.; Chu, S. G. *J. Appl. Polym. Sci.* **1986**, *32*, 5597.
(55) Han, C. D.; Jhon, M. S. *J. Appl. Polym. Sci.* **1986**, *32*, 3809.
(56) Han, C. D. *J. Appl. Polym. Sci.* **1988**, *35*, 167.
(57) The Doi–Edwards tube model was used for only a single relaxation time (i.e., $p = 1$) in ref 55, but eq 27 is valid for all odd values of p.
(58) Han, C. D.; Kim, J. K., unpublished research, 1987.
(59) Ferry, J. D. *Viscoelastic Properties of Polymers*, 3rd ed., Wiley: New York, 1980.
(60) Struglinski, M. J.; Graessley, W. W. *Macromolecules* **1985**, *18*, 2630.
(61) Masuda, T.; Kitagawa, K.; Onogi, S. *Polym. J. (Tokyo)* **1970**, *1*, 418.
(62) Graessley, W. W. *Adv. Polym. Sci.* **1974**, *16*, 1.
(63) Doi, M.; Edwards, S. F. *The Theory of Polymer Dynamics*; Clarendon Press: Oxford, 1986.
(64) Lifshitz, E. M.; Pitaevskii, L. P. *Statistical Physics*, 3rd ed.; Pergamon Press: Oxford, 1980; Part 1, p 377.

Characterization and Optical Anisotropy of Oligo- and Polystyrenes in Dilute Solutions

Toshiki Konishi, Takenao Yoshizaki, Jiro Shimada, and Hiromi Yamakawa*

Department of Polymer Chemistry, Kyoto University, Kyoto 606, Japan.
Received July 20, 1988; Revised Manuscript Received September 19, 1988

ABSTRACT: Mean-square optical anisotropies $\langle\Gamma^2\rangle$ were determined from anisotropic light scattering for atactic polystyrenes of narrow molecular weight distributions in cyclohexane at 34.5 °C and in carbon tetrachloride at 25 °C over a wide range of molecular weight, including the oligomer region. No appreciable differences were observed between the results for $\langle\Gamma^2\rangle$ in the two solvents. A preliminary consideration on the basis of the rotational isomeric state model for atactic polystyrene showed that $\langle\Gamma^2\rangle$ appreciably depends on the stereochemical composition. Thus the fractions of racemic dyads f_r in the samples were determined by ^{13}C NMR prior to the measurements and were found to be almost the same, ca. 0.59. From an analysis of the experimental data for $\langle\Gamma^2\rangle$ on the basis of the helical wormlike chain, its model parameters, i.e., the constant differential-geometrical curvature κ_0 and torsion τ_0 of the regular helix that its chain contour takes at the minimum of its potential energy, the stiffness parameter λ^{-1}, and the shift factor M_L (molecular weight per unit contour length), were determined for the atactic polystyrene of $f_r = 0.59$ as $\lambda^{-1}\kappa_0 = 3.0$, $\lambda^{-1}\tau_0 = 6.0$, $\lambda^{-1} = 22.7$ Å, and $M_L = 37.1$ Å^{-1}. Theoretical values of $\langle\Gamma^2\rangle$ calculated with these parameters well reproduced the data for $\langle\Gamma^2\rangle$ for $x \geq 5$ with x the degree of polymerization of the sample. The values of $\langle\Gamma^2\rangle$ calculated for the rotational isomeric state model coincided with the experimental results for $x \leq 4$ but deviated somewhat upward for $x > 5$.

I. Introduction

As far as the global properties of long flexible polymers are concerned, the Gaussian chain model provides a good theoretical basis for calculations of their dilute solution properties.[1] However, a more precise polymer model reflecting the details of the chain structure is needed to

0024-9297/89/2222-1921$01.50/0

predict the solution properties of short (oligomer) chains or those related to the local structure (i.e., individuality) of long chains. The rotational isomeric state (RIS) model[2,3] has been introduced for this purpose and applied with reasonable success to the evaluation of equilibrium properties such as characteristic ratios, mean-square radii of gyration, angular correlation functions, persistence vectors, and so forth for a variety of flexible polymers. Unfortunately, however, the RIS model is physically inadequate for the treatment of dynamic properties, and also is not amenable to mathematical treatments even for steady-state transport problems.

Thus we have presented a very general continuous model, now called the helical wormlike (HW) chain.[4,5] It is an elastic wire model with both bending and torsional energies and may be regarded as a generalization of the Kratky–Porod wormlike chain.[1,6] At the minimum of its elastic (potential) energy, the contour of the HW chain takes a regular helix defined by the constant differential-geometrical curvature κ_0 and torsion τ_0. Thus it can represent the equilibrium conformational behavior of real flexible polymers randomly possessing complete or incomplete helical conformations in solution. They may be traces of helices present in the crystalline state or spirals of relatively large radius arising from certain preferred conformations in the chain with different bond angles. In addition to κ_0 and τ_0, there are two other basic model parameters in the case of flexible chains; one is the stiffness parameter λ^{-1}, defined as the bending force constant divided by $^1/_2kT$ with k the Boltzmann constant and T the absolute temperature, and the other is the shift factor M_L, defined as the molecular weight per unit contour length.

On the basis of this new model, we have made extensive theoretical studies on equilibrium and dynamic properties of dilute solutions of flexible polymers.[4] Our results for the equilibrium properties have been favorably compared with the RIS calculations for various symmetric and asymmetric vinyl chains. This fact has allowed us to determine the four HW basic model parameters above for the relevant polymer chains. With the model parameters thus determined, we have given a consistent explanation of the dynamic (and steady-state transport) properties of flexible chains. Thus it can be said that the HW chain can mimic the conformational behavior of individual real chains on the bond length or somewhat longer scales, provided that the RIS method gives correct predictions for real polymers.

However, since the RIS model is not necessarily assured to represent real polymers accurately, it is desirable to directly compare the HW chain theory with true experimental data. For this purpose, we need the data over a wide range of molecular weight, including the oligomer region, obtained for the well-characterized polymer samples (in Θ solvents). We have recently shown that mean-square dipole moments,[7] mean-square radii of gyration,[8] and intrinsic viscosities[9] may well be explained by the HW chain with the model parameters determined from an analysis of the experimental data. However, the experimental data that meet the above requirements are scarcely found in literature. This is the motivation by which we have started a series of experimental studies on dilute solution properties of flexible polymers, including the oligomers.

The present paper deals with the mean-square optical anisotropy $\langle\Gamma^2\rangle$ for atactic oligo- and polystyrenes (a-PS). In order to obtain $\langle\Gamma^2\rangle$, we measure the depolarized component R_{Hv} of the reduced scattering which is determined experimentally as the ratio of the horizontal component of the scattered intensity per unit volume to the intensity of vertically polarized incident light. It is known that R_{Hv} consists of two parts,[10] the intrinsic molecular one $R_{Hv,mol}$ and collision-induced one $R_{Hv,col}$, and $\langle\Gamma^2\rangle$ must be determined from the former. Flory and his co-workers[11-14] made a systematic study on $\langle\Gamma^2\rangle$ for various polymers both theoretically and experimentally. In the study on a-PS,[13] they determined $R_{Hv,mol}$ and $R_{Hv,col}$ separately from R_{Hv}, using the correction procedure devised by Carlson and Flory.[15] The values of $\langle\Gamma^2\rangle$ determined from $R_{Hv,mol}$ thus obtained were shown to have a good correlation with the RIS values calculated with the RIS model parameters.[16] Thus we must also make this correction. We already extended their procedure to the case for which a mercury lamp is used in place of laser as the light source.[17]

Table I
Terminal Groups of R(-$CH_2CHPh)_x$-R′

type	R	R′
a	a-PS chain	a-PS chain
b	H	CH_3
c	C_4H_9	H

Further, we must consider the fact that solution properties of an asymmetric vinyl polymer may depend appreciably on the stereochemical composition (as expressed by the fraction f_r of racemic dyads). However, experimental studies reported so far on the solution properties of a-PS have not paid due attention to this fact and the fundamental importance of the quantity f_r. In this work, we determined f_r of all the PS samples by means of ^{13}C NMR prior to measurements of their solution properties.

The main purposes of the present study are thus 2-fold: (1) to determine the HW model parameters from an analysis of the experimental data and (2) to examine the RIS predictions, using a-PS samples well characterized for both the molecular weight distribution and the stereochemical composition.

Before proceeding to the Experimental Section, in the next section we examine the dependences of $\langle\Gamma^2\rangle$ and the mean-square radius of gyration $\langle S^2\rangle$ on the stereochemical composition (or tacticity) on the basis of the RIS model. We note that although Suter and Flory[13] have carried out RIS calculations of $\langle\Gamma^2\rangle$, they have not shown its precise dependences on the chain length and stereochemical composition f_r. We also examine the dependence of $\langle\Gamma^2\rangle$ on terminal groups, since our PS samples and those used by Suter and Flory[13] have different terminal groups.

II. Preliminary Consideration with the RIS Model

We consider three types (a, b, and c) of a-PS chains as shown in Table I. The type-a chain is a subchain contained in an infinitely long chain, and there is no end effect on it. The type-b chain has methyl groups on both ends. Flory and his co-workers[13,18] treated only this type of chain on the basis of the RIS model. The type-c chain (i.e., α-hydro-ω-butylpolystyrene) is the one synthesized by anionic polymerization with *n*-butyllithium as an initiator. Note that our samples and most of the samples used in recent experiments are of this type.

In order to carry out the RIS calculations of $\langle S^2\rangle$ and $\langle\Gamma^2\rangle$ for these chains, we need values of the statistical weights for the first-order and second-order interactions, supplements $\hat{\theta}$ of skeletal bond angles, rotation angles $\hat{\varphi}$, a skeletal bond length l, bond and group polarizability tensors, and other bond angles determining the orientation of side groups. For the type-a and -b chains, we can use the RIS model parameters determined by Flory and his co-workers.[2,13,15,18] However, the type-c chain requires a special consideration, since it may be regarded as a

methylene–styrene diblock copolymer, its terminal group in the styrene block being not a methyl group but a hydrogen atom. No values are available for the RIS model parameters in the neighborhood of the junction point of the two blocks and at the terminal of the styrene block.

For the styrene block, we adopt the new Flory convention[19] to describe the stereochemical configuration of the asymmetric chain. Let $\sigma\eta$, σ, and $\sigma\tau$ (=0) be the statistical weights for the first-order interaction for the t, g, and $\bar{g}$ conformations, respectively. Note that $\bar{g}$ is inhibited, and that the parameter σ is set equal to unity, for simplicity. As for the pair of bonds flanking an α carbon C^α, the statistical weight $\omega_{\alpha\alpha}$ for the second-order interaction for $C^\alpha\cdots C^\alpha$ is assumed to be zero, considering the inevitable higher order interaction between the phenyl groups (Ph). As for the pair of bonds between successive C^αs, the weights for the second-order interactions are denoted by $\omega = \omega_{MM}^{(S)}$ for Me$\cdots$Me, by ω' for Me$\cdots$Ph, and by ω'' for Ph$\cdots$Ph, where Me denotes CH_2 or CH_3.

The values of the parameters adopted for the styrene block are the following: $\hat{\theta}'$ (at the CH_2) = 66°, $\hat{\theta}''$ (at the C^α) = 68°, $\hat{\varphi}$ = 10° (t) and 110° (g), l = 1.53 Å, $\omega = \omega'$ = 0.0504, ω'' = 0.0492, and η = 1.54. These statistical weights have been calculated at 34.5 °C (Θ temperature for a-PS in cyclohexane), following Yoon et al.[16]

For the methylene block, let 1 and σ' be the statistical weights for the first-order interactions for the t and $g^\pm$ conformations, respectively, and let $\omega_{MM}^{(M)}$ be the weight for the second-order interaction for $CH_2\cdots CH_2$. The values of the parameters adopted are the following: $\hat{\theta}$ = 68°, $\hat{\varphi}$ = 0° (t), 120° (g^+), and −120° (g^-), σ' = 0.441, and $\omega_{MM}^{(M)}$ = 0.0379. These values for σ' and $\omega_{MM}^{(M)}$ have also been calculated at 34.5 °C, following Flory.[2,20]

Next we consider the RIS model parameters in the neighborhood of the junction point of the two blocks and at the terminal of the styrene block (in the type-c chain). We number the skeletal bonds serially from the butyl end, regarding $CH_3\rightarrow CH_2$ as the first skeletal bond. We also number the skeletal carbons from 0 to $2x + 3$ with x the degree of polymerization, i.e., the number of the phenyl groups. It is convenient to regard one of the C^α–H bonds at the terminal as the $(2x + 4)$th virtual skeletal bond.

For the pairs of bonds (3, 4) and (5, 6) in the neighborhood of the junction point, a new parameter $\omega_{M\alpha}$ is required to represent the second-order interaction for $CH_2\cdots C^\alpha$. Its value may be expected to be intermediate between $\omega_{MM}^{(S)}$ for $CH_2\cdots CH_2$ and $\omega_{\alpha\alpha}$ (=0) for $C^\alpha\cdots C^\alpha$. For the pair of bonds (4, 5), a parameter $\bar{\omega}_{MM}$ for the second-order interaction for $CH_2\cdots CH_2$ may be equated to a mean of $\omega_{MM}^{(M)}$ for the methylene block and $\omega_{MM}^{(S)}$ for the styrene block. We assume that the other parameters required for the 4th to 6th bonds are not perturbed by the presence of the junction point.

At the terminal of the styrene block, it is necessary to consider the orientation of the phenyl group attached to the final C^α. Inside the styrene block, the phenyl ring is taken to be perpendicular to the plane determined by the successive skeletal bonds $CH_2\rightarrow C^\alpha$ and $C^\alpha\rightarrow CH_2$. However, at the terminal the ring may be expected to be nearly perpendicular to the plane determined by the $(2x + 2)$th and $(2x + 3)$th bonds [but not to the $(2x + 4)$th virtual skeletal bond $C^\alpha\rightarrow H$], considering the steric hindrance between the phenyl groups. Thus we introduce a new parameter $\hat{\omega}_{\alpha\alpha}$ associated with the pair of bonds $(2x + 1, 2x + 2)$ for the second-order interaction for $C^\alpha\cdots C^\alpha H_2$ (at the terminal). Its value may be expected to be intermediate between $\omega_{\alpha\alpha}$ = 0 and $\omega_{MM}^{(S)}$. In the particular case of x = 1 or 2, we must introduce a parameter $\hat{\omega}_{M\alpha}$ for the second-order interaction for $CH_2\cdots C^\alpha H_2$ (at the terminal). Its value may be expected to be intermediate between $\omega_{\alpha\alpha}$ = 0 and $\omega_{MM}^{(M)}$. The orientation of the terminal phenyl ring may also affects the other RIS model parameters, e.g., ω' and ω''. However, we do not consider the changes of these parameters, for simplicity, since it is difficult to estimate them without detailed conformational energy calculations. (The change in the polarizability tensor associated with the orientation of the terminal phenyl group must be taken into account.)

The final expressions for the statistical weight matrix $\mathbf{U}_j^{(x)}$ for the pair of bonds $(j - 1, j)$ for the x-mer of the type-c chain are given in the Appendix. In these expressions, we have formally regarded the first, third, and final skeletal carbons as the "asymmetric" carbons and treated the dyads in the methylene block and the final dyad as "meso", for convenience.

As for the bond rotation angles $\hat{\varphi}$, we use the values in the methylene block for the 4th bond ($CH_2\rightarrow CH_2$) and the $(2x + 3)$th bond and the values in the styrene block for the 5th bond ($CH_2\rightarrow C^\alpha$).

The (traceless) polarizability tensor α_{ij} for a cylindrically symmetric bond connecting atoms i and j may be expressed as the diagonal matrix

$$\alpha_{ij} = \Delta\alpha_{ij}\ \mathrm{diag}\ (2/3, -1/3, -1/3) \qquad (1)$$

where $\Delta\alpha_{ij} = \alpha_{ij\parallel} - \alpha_{ij\perp}$ (the anisotropy of the bond $i\rightarrow j$) with $\alpha_{ij\parallel}$ and $\alpha_{ij\perp}$ being the polarizabilities parallel and perpendicular to the bond, respectively, and the first reference axis is in the direction of the cylinder axis. The bond polarizabilities adopted are[11-13]

$$\Delta\alpha_{CC} = 0.95\ \text{Å}^3, \qquad \Delta\alpha_{CH} = 0.21\ \text{Å}^3 \qquad (2)$$

Further, the polarizability tensor α_{Ph} adopted for the group C^α–Ph is[13]

$$\alpha_{Ph} = \mathrm{diag}\ (3.06,\ -3.03,\ -0.03)\ \text{Å}^3 \qquad (3)$$

where the first reference axis is in the direction of the $C^\alpha\rightarrow$Ph bond, the second is perpendicular to the plane of the phenyl ring, and the third completes a right-handed Cartesian coordinate system.

We carried out the RIS calculations of $\langle\Gamma^2\rangle$ and $\langle S^2\rangle$ by the Monte Carlo method established by Flory and his co-workers,[2] where $\langle S^2\rangle$ was computed assuming that the same mass is placed at all the skeletal carbons. It was found that the results for the type-c chain are insensitive to change in the values of the parameters $\omega_{M\alpha}$, $\omega_{\alpha\alpha}$, and $\hat{\omega}_{M\alpha}$ within their plausible ranges. Thus the values assigned are $\bar{\omega}_{MM} = (\omega_{MM}^{(M)} + \omega_{MM}^{(S)})/2 = 0.0441$, $\omega_{M\alpha} = \hat{\omega}_{\alpha\alpha} = (\omega_{\alpha\alpha} + \omega_{MM}^{(M)})/2 = 0.0190$, and $\hat{\omega}_{M\alpha} = \omega_{MM}^{(M)} = 0.0379$.

Figures 1 and 2 show plots of the ratio $\langle\Gamma^2\rangle/x$ against the logarithm of x and the ratio $\langle S^2\rangle/nl^2$ against the logarithm of n, respectively, for the type-c a-PS chains with the indicated values of f_r, where n $(=2x + 3)$ is the number of (real) skeletal bonds. The number of Monte Carlo chains generated is so large (300–2000) that the statistical fluctuations in the values of $\langle\Gamma^2\rangle$ and $\langle S^2\rangle$ are less than 1%. It is seen that for $x > 3$, both the ratios increase monotonically to their constant coil limiting values as x or n is increased. The ratios are sensitive to change in f_r; their coil limiting values first decrease and then increase as f_r is increased from 0 to 1, and they vary by 15–25% when f_r increases from 0.4 to 0.6. This indicates that if f_r changes with chain length, the dependences of $\langle\Gamma^2\rangle$ and $\langle S^2\rangle$ on chain length become quite different from those with fixed f_r. Thus experimental studies on solution properties of a-PS should be made by using a series of samples of different molecular weights but with the same stereochemical composition.

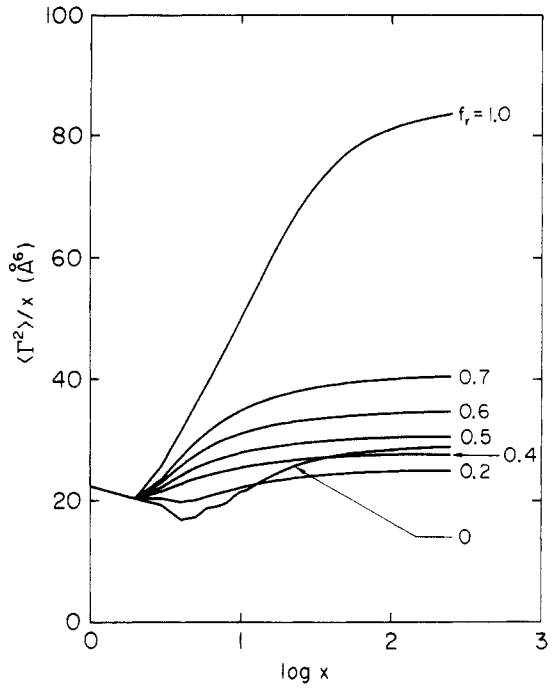

Figure 1. RIS values of $\langle\Gamma^2\rangle/x$ plotted against the logarithm of the degree of polymerization x for the type-c a-PS chains. The attached numbers indicate the values of the fraction of racemic dyads f_r.

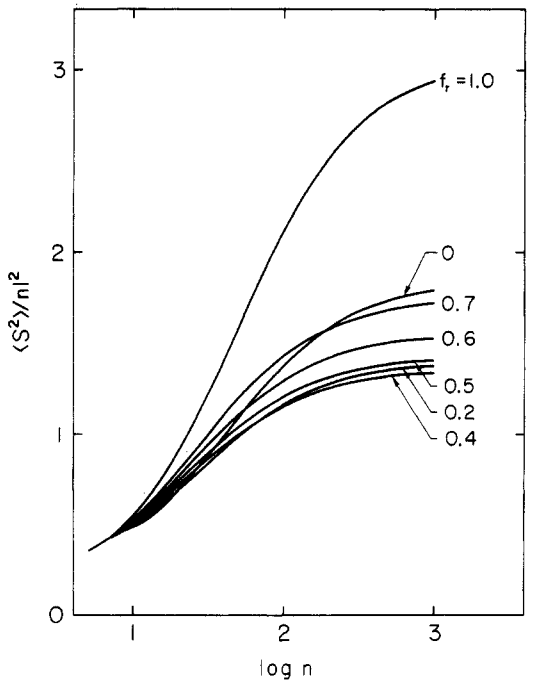

Figure 2. RIS values of $\langle S^2\rangle/nl^2$ plotted against the logarithm of the number of the skeletal bonds n for the type-c a-PS chains. The attached numbers indicate the values of f_r.

The ratios $\langle\Gamma^2\rangle/x$ and $\langle S^2\rangle/nl^2$ for the type-a, -b, and -c a-PS chains with $f_r = 0.6$ are plotted in Figure 3. It is seen that the end effect is appreciable for $\langle\Gamma^2\rangle$ for small x but small for $\langle S^2\rangle$ over the whole range of x.

III. Experimental Section

Materials. The α-hydro-ω-butyloligostyrene and -polystyrene samples used in this work were commercial ones (prepared by anionic polymerization with n-butyllithium as an initiator) supplied from the Tosoh Co., Ltd., by the courtesy of Dr. M. Fukuda. The oligostyrene samples designated A-500 and A-1000 by the company were separated into x-mers (x = 3, 4, 5, 6, and 8) by gel permeation chromatography (GPC). The separation was performed with two serially connected Tosoh G2000H6 (600 × 50 mm) columns using chloroform as an eluent at a flow rate of 17 mL/min. The oligostyrene samples of 3-, 4-, 5-, 6-, and 8-mers thus obtained were designated OS3, OS4, OS5, OS6, and OS8, respectively. The original samples designated A-2500, A-5000, F-1, and F-128 by the company were separated into fractions by fractional precipitation using benzene as a solvent and methanol as a precipitant. The sample A-2500 was first divided into five fractions, and then the second and fifth fractions were further divided into three fractions. The respective middle fractions A2500-a and A2500-b were used as test samples for the present measurements. The sample A-5000 was divided into four fractions, and the samples F-1 and F-128 were divided into three fractions. The third fraction of A-5000 and the middle fractions of F-1 and F-128 were chosen as test samples and were designated A5000-3, F1-2, and F128-2. The samples OSx were dissolved in chloroform, filtered through a ultracellafilter membrane with pore size of 0.45 μm, and then dried under vacuum at 50 °C. The samples A2500-a, A2500-b, A5000-3, F1-2, and F128-2 were freeze-dried from their benzene solutions after filtration through the membrane.

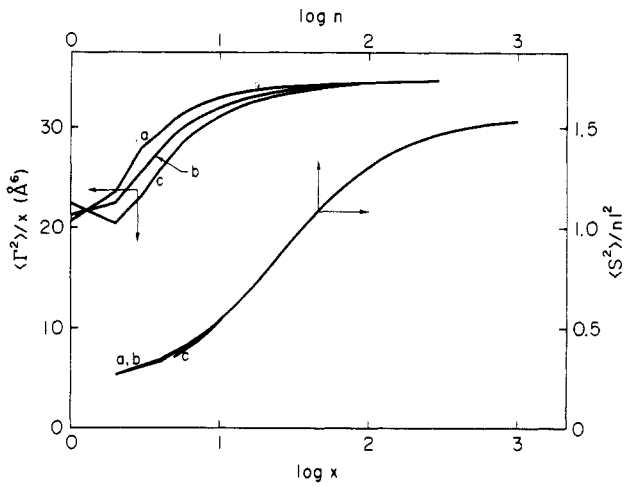

Figure 3. RIS values of $\langle\Gamma^2\rangle/x$ and $\langle S^2\rangle/nl^2$ plotted against the logarithm of x and n, respectively, for the type-a, -b, and -c a-PS chains with f_r = 0.6.

Solvents and cumene used for light-scattering measurements were purified according to the standard procedure. Solvents used for taking ^{13}C NMR spectra were of reagent grade.

^{13}C NMR. ^{13}C NMR spectra of aliphatic carbons of the samples OS5, OS6, F1-2, and F128-2 were recorded on a JEOL JNM GX-400 spectrometer at 100.5 MHz. The spectra were taken for 1,2-dichlorobenzene solutions containing perdeuteriobenzene for a signal lock at 120 °C. The chemical shifts referred to the 4-carbon of 1,2-dichlorobenzene (127.3 ppm) were converted to the TMS scale. An rf pulse angle of 90° which corresponds to 9.3 μs was used. The pulse repetition time was 10 s, which is more than five times as long as the longest spin–lattice relaxation time T_1 of aliphatic carbon atoms under observation. The spectral width was 20 kHz and 32K data tables were used. The gated proton decoupling method was employed. The sample concentrations were in the range from 10 to 20 wt %.

Light Scattering. Light-scattering measurements were carried out for methyl ethyl ketone (MEK) solutions at 25 °C, cyclohexane solutions at 34.5 °C (Θ temperature), and carbon tetrachloride (CCl_4) solutions at 25 °C with a Fica 50 automatic light-scattering photometer (with a mercury lamp as the light source). The photometer had been modified to be suitable for the correction of the collision-induced polarizability in the manner reported before.[17] For calibration of the apparatus, the intensity of light scattered from pure benzene was measured at 25 °C at scattering angle θ of 90° with the incident light of wavelength 436 nm, where the Rayleigh ratio of pure benzene was taken as 46.5×10^{-6} cm^{-1} under these conditions. The depolarization ratio ρ_u of pure benzene was determined to be 0.43 under the same conditions by the method of Rubingh and Yu. In order to obtain the calibrative constants for the solvents used for the measurements, the $\tilde{n}^2$ correction of Hermans[21] was applied, where $\tilde{n}$ is the refraction index of the solvent. For the values of $\tilde{n}$ at wavelength

Table II
Values of x_w, M_w, and M_w/M_n for Samples OSx

sample	x_w	M_w	M_w/M_n
OS3	3	370	1.00
OS4	4	474	1.00
OS5	5	578	1.00
OS6	5.9_8	680	1.00
OS8	8.1_3	904	1.01

Table III
Values of M_w, x_w, and M_w/M_n for Samples Other Than OSx

sample	$10^{-3}M_w$	x_w	M_w/M_n
A2500-a	2.2_7	$21._2$	1.05
A2500-b	3.4_8	$32._9$	1.07
A5000-3	5.3_8	$51._2$	1.03
F1-2	9.1[a]	87	1.03
F128-2	1260[a]	12100	

[a] Manufacturer's data for the original samples supplied from Tosoh Co., Ltd.

of 436 nm, we used 1.520 for benzene at 25 °C, 1.385 for MEK at 25 °C, 1.428 for cyclohexane at 34.5 °C, and 1.469 for CCl_4 at 25 °C.

The most concentrated test solution of each sample in cyclohexane was prepared by continuous stirring for 1–3 days at ca. 45 °C. Those in MEK and CCl_4 were continuously stirred for 1 day at room temperature. These solutions and the solvents were optically purified by filtration through ultracellafilter membranes with a pore size of 0.45 or 0.22 μm. Solutions of lower concentrations were obtained by successive dilution. Their concentrations were determined gravimetrically.

All measurements were carried out with vertically polarized incident light of wavelength 435.8 nm whose spectral distribution was sharpened by the use of a narrow band pass filter with full width at half-maximum (FWHM) of 0.9 nm. For the determination of $\langle\Gamma^2\rangle$, the excess H_V component ΔR_{Hv} of the reduced scattering was measured through a narrow band pass filter of central wavelength 435.8 nm and FWHM = 0.9 or 2.5 nm for cyclohexane and CCl_4 solutions of four or five concentrations at scattering angle $\theta = 90°$. The transmittance of each filter as a function of wavenumber is approximately Gaussian. The square root of its variance is 28 cm^{-1} ($=\sigma_1$) for FWHM = 0.9 nm and 79 cm^{-1} ($=\sigma_2$) for FWHM = 2.5 nm.

In order to determine the molecular weights of A2500-a, A2500-b, and A5000-3, we measured R_{Uu} and R_{Uv} for their MEK solutions of four or five concentrations at scattering angles ranging from 30° to 142.5°. Here, the subscripts U and u indicate the unpolarized incident and scattered light, respectively. Refractive index increments of these PS samples in MEK were measured at 25.0 °C by using a Shimadzu differential refractometer. The scattering data for the determination of the molecular weights were analyzed following the procedure of Zimm and Berry.

IV. Results

Molecular Weights and Their Distributions. It was found from the GPC diagrams of the oligostyrene samples OSx (x = 3, 4, 5, 6, and 8) that OS3, OS4, and OS5 were completely monodisperse, and that OS6 contained 5.6 wt % 5-mer and 5.2 wt % 7-mer and OS8 contained 18.4 wt % 7-mer and 31.7 wt % 9-mer. The values of the weight-average degree of polymerization x_w, the weight-average molecular weight M_w, and the ratio of M_w to the number-average molecular weight M_n for these samples are listed in Table II. In Table III are given the values of M_w determined from the light-scattering measurements, x_w calculated from M_w, and M_w/M_n determined from GPC for the samples A2500-a, A2500-b, and A5000-3, together with those for the samples F1-2 and F128-2. The values of M_w for the latter two are manufacturer's data for the original samples from Tosoh Co., Ltd. The molecular weight distributions of the samples are narrow enough for our present work.

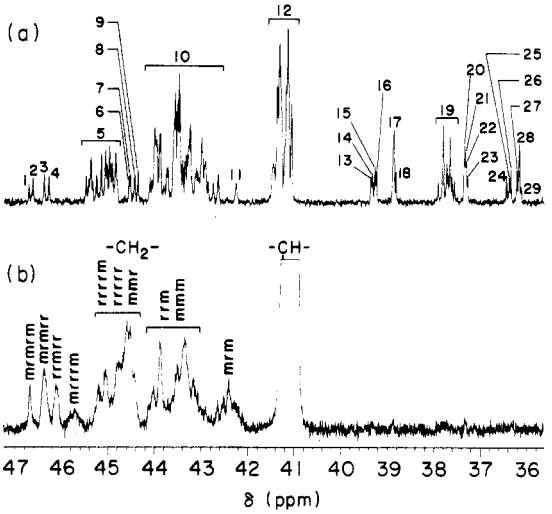

Figure 4. ^{13}C NMR spectra of aliphatic carbons of the samples OS6 (a) and F1-2 (b): m = meso and r = racemic.

Stereochemical Compositions. In a previous work,[22] we had already determined the fractions of racemic dyads f_r of the samples OS4 and OS5. In the same manner, we determined f_r of the sample OS6 from the ^{13}C NMR spectra. We first evaluated the chemical shifts δ of aliphatic carbons in the stereoisomers of the 6-mer. The chemical shift of a given aliphatic carbon in a stereoisomer of a given conformation consists of the chemical shift δ^* for the trans planar conformation and the chemical shift $\Delta\delta$ relative to δ^*, which depends on the conformation. Thus the observed chemical shift δ of the carbon of the stereoisomer may be expressed as $\delta = \delta^* + \langle\Delta\delta\rangle$, where $\langle\ \rangle$ denotes an equilibrium conformational average. We calculated $\langle\Delta\delta\rangle$ on the basis of the RIS model taking account of the γ effect[23] and estimated δ^* from the results for the 5-mer. The values of δ thus obtained are listed in Table IV. With these values, we made assignments of the spectra shown in Figure 4a. The results are also listed in Table IV, where C-j indicates the jth aliphatic (or skeletal) carbon. [In ref 22, the aliphatic carbons were numbered from the opposite (hydrogen) end.] Assuming the stereoisomer distribution in the a-PS chain to be Bernoullian, we finally determined f_r so that the root-mean-square deviation of the calculated intensities from the observed ones becomes a minimum. The value of f_r thus determined for the sample OS6 was 0.57. The observed and calculated intensities are also given in Table IV.

For the ^{13}C NMR spectra of the samples F1-2 and F128-2, we used the peak assignments given by Sato et al.,[24] as shown in Figure 4b. The values of f_r were determined to be 0.59 for both samples, in the same manner as in the case of the sample OS6. We note that the absorption by the aliphatic carbons near the ends of a-PS chain was taken into account for the sample F1-2. For the ^{13}C NMR spectra for the sample OS3, which had already been recorded, the peak assignments given by Ray et al.[25] were used and the value of f_r was determined to be 0.57.

In Table V are given the values of f_r determined above together with those obtained previously[22] for the samples OS4 and OS5. The values of f_r are almost the same for all the samples examined and may be set equal to 0.59.

Determination of Mean-Square Optical Anisotropies $\langle\Gamma^2\rangle$. The concentration dependences of $\Delta R_{Hv}(\sigma_i)/c$ (i = 1 and 2) for cyclohexane solutions of the a-PS samples (circles) and cumene (triangles) are shown in Figures 5 and 6. Here, σ_i (i = 1 and 2) denotes the type of the narrow band pass filter through which ΔR_{Hv} was measured. The

Table IV
Observed and Calculated Values of ^{13}C NMR Chemical Shifts and Intensities of the Sample OS6

$$\overset{0}{C}H_3\overset{1}{C}H_2\overset{2}{C}H_2\overset{3}{C}H_2\overset{4}{C}H_2\overset{5}{C}H(C_6H_5)\overset{6}{C}H_2\overset{7}{C}H(C_6H_5)\overset{8}{C}H_2\overset{9}{C}H(C_6H_5)\overset{10}{C}H_2\overset{11}{C}H(C_6H_5)\overset{12}{C}H_2\overset{13}{C}H(C_6H_5)\overset{14}{C}H_2\overset{15}{C}H_2(C_6H_5)$$

peak	assignment	δ, ppm obsd	δ, ppm calcd	intensity, % obsd	intensity, % calcd	peak	assignment	δ, ppm obsd	δ, ppm calcd	intensity, % obsd	intensity, % calcd
1	C-10 rmrm* [a,b]	46.71	46.42	0.31	0.51	11	C-10 mrmm	42.25	41.93	0.71	0.78
2	C-8 mrmr*	46.62	46.42	0.62	0.61		C-8 mmrm				
3	C-10 rmrr**	46.38	46.18	0.59	0.68	12	C-7	41.46			
4	C-8 rrmr**	46.28	46.18	0.62	0.68		C-9	|	41.31	27.42	26.98
5	C-10 rrrα [c]						C-11	41.07			
	C-8 αrrr					13	C-14 rmmm	39.36	39.46	0.99	0.97
	C-12 mrαβ					14	C-14 rmmr	39.33	39.41		
	C-6 αβrm					15	C-14 rmrr	39.27	39.32	1.39	1.29
		45.48	45.85								
	C-10 rmmα	|	|	11.22	11.55	16	C-14 rmrm	39.24	39.30		
	C-8 αmmr	44.85	44.85			17	C-14 rrrm		39.07		
								38.89			
	C-10 mmrα						C-14 rrrr	|	39.05	3.22	2.99
								38.87			
	C-8 αrmm						C-14 rrmr		38.99		
6	C-12 rrmm	44.56	44.71	0.93	1.03	18	C-14 rrmm	38.82	38.96		
7	C-6 mmrr	44.53	44.66			19	C-14 mαβγ	37.91	38.03		
								|	|	5.89	6.22
8	C-12 rrmr	44.43	44.56	0.81	0.87		C-4 αβmr	37.57	37.17		
9	C-6 rmrr	44.36	44.51	0.62	0.68	20	C-4 rrrr	37.36	37.55		
10	C-10 mmmα					21	C-4 mrrr	37.34	37.57	2.85	2.99
	C-8 αmmm					22	C-4 rmrr	37.32	37.49		
	C-12 αmβγ					23	C-4 mmrr	37.28	37.46		
	C-6 αβmγ					24	C-4 rmrm	36.44	36.48	0.53	0.51
	C-10 mrrα					25	C-4 mmrm	36.39	36.52	0.99	1.21
	C-8 αrrm					26	C-4 rrrm	36.35	36.39		
	C-12 rrrα	44.11	44.46			27	C-4 mrrm	36.22	36.37		
		|	|	37.84	37.23					
	C-10 rrmα	42.64	42.13			28	C-4 mrmm		35.99	2.45	2.24
	C-8 αmrr						C-4 rrmm	36.17	35.94		
	C-6 αrrr						C-4 rmmm		35.77		
	C-5					29	C-4 mmmm	36.12	35.66		
	C-13										
	C-10 mrmr										
	C-8 rmrm										

[a] m = meso; r = racemic. [b] Assignments indicated by the same superscript can be interchanged. [c] The symbol rrrα abbreviates rrr*m* and rrr*r*; mrαβ abreviates mr*mm*, mr*mr*, mr*rm*, and mr*rr*; and so on.

Table V
Values of f_r Determined from ^{13}C NMR Spectra

sample	f_r	sample	f_r
OS3	0.57	OS6	0.57
OS4	0.60[a]	F1-2	0.59
OS5	0.58[a]	F128-2	0.59

[a] See ref 22.

Table VI
Results of Light-Scattering Measurements on Atactic Oligo- and Polystyrenes in Cyclohexane at 34.5 °C

sample	$10^6 \times [\Delta R_{Hv}(\sigma_1)/c]_{c=0}$, cm²/g	$10^6 \times [\Delta R_{Hv}(\sigma_2)/c]_{c=0}$, cm²/g	$\Delta R_{Hv,col}/\Delta R_{Hv,total}$	$\langle\Gamma^2\rangle/x$, Å⁶
cumene	3.37	6.58	0.51	21.3 ± 3
OS3	3.47	6.83	0.54	21.5 ± 1
OS4	3.85	7.44	0.48	25.1 ± 1
OS5	4.17	8.05	0.49	26.4 ± 2
OS6	4.43	8.53	0.47	28.4 ± 2
OS8	4.76	9.22	0.49	28.8 ± 1
A2500-a	5.22	10.08	0.48	30.8 ± 1
A2500-b	5.41	10.53	0.51	30.2 ± 3
A5000-3	6.17	12.20	0.56	31.4 ± 3

data points for each sample follow a straight line and can be easily extrapolated to obtain $[\Delta R_{Hv}(\sigma_i)/c]_{c=0}$, except for the samples A2500-a, A2500-b, and A5000-3. The data for these three samples were extrapolated to zero concentration by smooth curves, as shown in the figures. The extrapolated values for these samples thus involve larger uncertainties than the others. The $\Delta R_{Hv}(\sigma_i)/c$ versus c plots for CCl_4 solutions are linear for all the samples studied, as shown in Figures 7 and 8. The values of $[\Delta R_{Hv}(\sigma_i)/c]_{c=0}$ estimated from these plots are listed in the second and third columns of Tables VI and VII.

Table VII
Results of Light-Scattering Measurements on Atactic Oligo- and Polystyrenes in Carbon Tetrachloride at 25 °C

sample	$10^6 \times [\Delta R_{Hv}(\sigma_1)/c]_{c=0}$, cm²/g	$10^6 \times [\Delta R_{Hv}(\sigma_2)/c]_{c=0}$, cm²/g	$\Delta R_{Hv,col}/\Delta R_{Hv,total}$	$\langle\Gamma^2\rangle/x$, Å⁶
cumene	3.09	5.94	0.46	19.8 ± 2
OS3	3.31	6.39	0.48	21.4 ± 2
OS4	3.63	6.96	0.46	23.2 ± 1
OS5	4.04	7.70	0.44	25.8 ± 1
OS6	4.17	7.96	0.44	26.0 ± 1
A2500-a	5.15	9.94	0.48	28.7 ± 2
A2500-b	5.06	9.74	0.47	28.3 ± 1
A5000-3	5.42	10.42	0.47	30.3 ± 1

As reported before,[17] even if the incident light has spectral distribution, $\Delta R_{Hv}(\sigma_1)$ and $\Delta R_{Hv}(\sigma_2)$ are related to $\Delta R_{Hv,mol}$ and $\Delta R_{Hv,col}$ as

$$\Delta R_{Hv}(\sigma_i) = A(\sigma_i)\Delta R_{Hv,mol} + B(\sigma_i)\Delta R_{Hv,col} \qquad (i = 1, 2) \tag{4}$$

where $A(\sigma_i)$ and $B(\sigma_i)$ are the coefficients which depend on the spectral distribution of incident light, the spectral distributions of the intrinsic molecular and collision-induced scattered light for monochromatic incident light, and

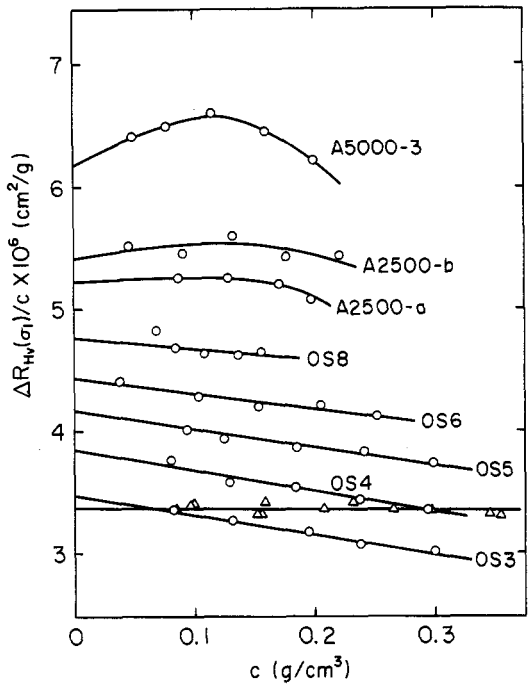

Figure 5. $\Delta R_{Hv}(\sigma_1)/c$ (with the band pass filter of $\sigma_1 = 28$ cm^{-1}) plotted against concentration c for a-PS samples (circles) in cyclohexane at 34.5 °C. The triangle represents the data for cumene.

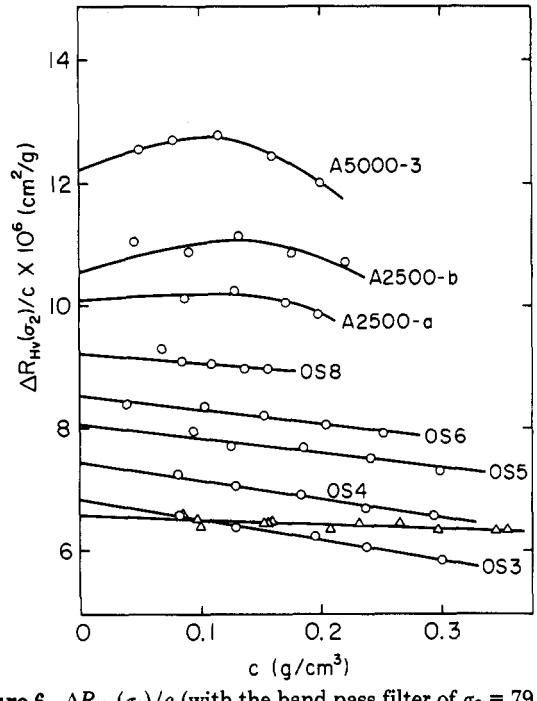

Figure 6. $\Delta R_{Hv}(\sigma_2)/c$ (with the band pass filter of $\sigma_2 = 79$ cm^{-1}) plotted against concentration c for a-PS samples in cyclohexane at 34.5 °C; see legend for Figure 5.

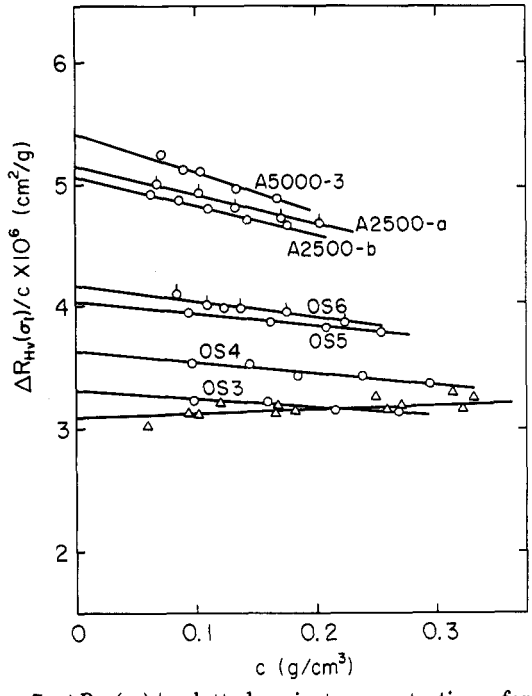

Figure 7. $\Delta R_{Hv}(\sigma_1)/c$ plotted against concentration c for a-PS samples in carbon tetrachloride at 25 °C; see legend for Figure 5.

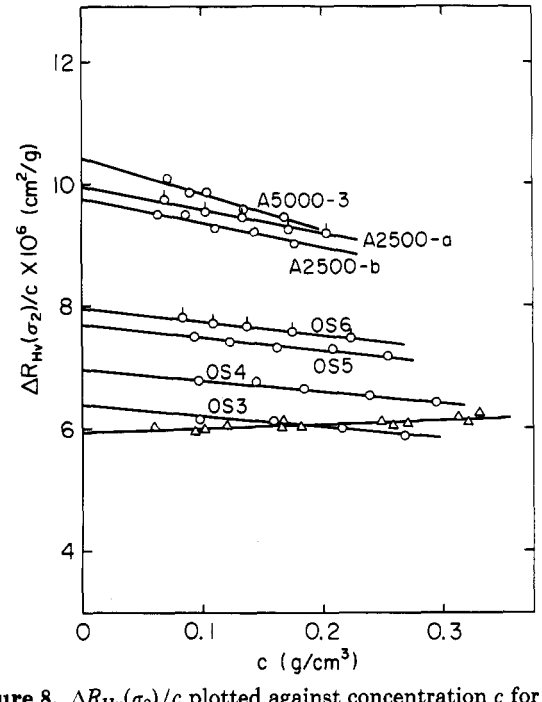

Figure 8. $\Delta R_{Hv}(\sigma_2)/c$ plotted against concentration c for a-PS samples in carbon tetrachloride at 25 °C; see legend for Figure 6.

the transmission curves of the filters. We determined the values of $A(\sigma_i)$ and $B(\sigma_i)$ so that the value of the ratio $\Delta R_{Hv,col}/\Delta R_{Hv,total}$ ($\Delta R_{Hv,total} = \Delta R_{Hv,mol} + \Delta R_{Hv,col}$) obtained for cumene in CCl_4 at 25 °C with our photometer agreed with the value 0.46 determined by Suter and Flory.[13] We note that although the wavelengths of our and their incident light are different (435.8 and 632.8 nm), we neglect the possible effects of the dispersion on ΔR_{Hv}. With these values, eq 4 gives

$$\Delta R_{Hv,mol} = 10.31\Delta R_{Hv}(\sigma_1) - 4.44\Delta R_{Hv}(\sigma_2) \quad (5)$$

$$\Delta R_{Hv,col} = -11.74\Delta R_{Hv}(\sigma_1) + 6.91\Delta R_{Hv}(\sigma_2) \quad (6)$$

We evaluated $[\Delta R_{Hv,mol}/c]_{c=0}$ and $[\Delta R_{Hv,col}/c]_{c=0}$ from eq 5 and 6 with the values of $[\Delta R_{Hv}(\sigma_i)/c]_{c=0}$ determined above. Here, we note that the ratio $\Delta R_{Hv,col}/\Delta R_{Hv,total}$ was almost independent of concentration. The values of this ratio do not change significantly with the samples examined, as seen from Tables VI and VII.

The mean-square optical anisotropy $\langle\Gamma^2\rangle$ is then calculated from

$$\langle\Gamma^2\rangle = \frac{15\lambda_0^4}{16\pi^4}\frac{M}{N_A}\left(\frac{3}{\tilde{n}^2+2}\right)^2[\Delta R_{Hv,mol}/c]_{c=0} \quad (7)$$

with the observed value of $[\Delta R_{Hv,mol}/c]_{c=0}$, where λ_0 is the wavelength of the incident light in vacuum, M the solute

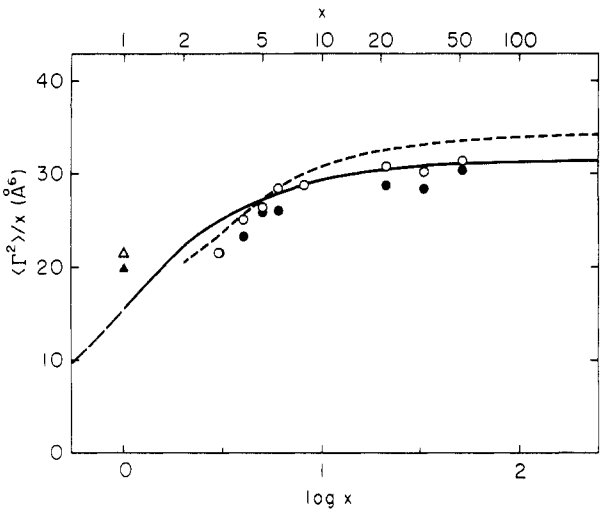

Figure 9. $\langle\Gamma^2\rangle/x$ plotted against log x for a-PS: (○) in cyclohexane at 34.5 °C; (●) in carbon tetrachloride at 25 °C. The triangles represent the data for cumene: (△) in cyclohexane at 34.5 °C; (▲) in carbon tetrachloride at 25 °C. The solid and dashed curves represent the HW theoretical values and the RIS values for f_τ = 0.59, respectively.

molecular weight, and N_A the Avogadro number, and the factor $[3/(\tilde{n}^2 + 2)]^2$ takes into account the effect of the internal field by the Lorenz-Lorentz relation. This relation requires some comments. No exact expression for the internal field effect is yet known. We have adopted the above factor for the following reasons: (1) In the present work, the values of $A(\sigma_i)$ and $B(\sigma_i)$ have been determined by the use of the values of $\Delta R_{\mathrm{Hv,mol}}$ and $\Delta R_{\mathrm{Hv,col}}$ evaluated by Suter and Flory[13] for cumene in CCl_4 at 25 °C with the above factor, and (2) in the theoretical calculation of $\langle\Gamma^2\rangle$, we employ the bond and group polarizability tensors evaluated by the use of the same factor. Moreover, the effect of internal field is immaterial as far as the chain length dependence of the optical anisotropy is concerned.

The values of $\langle\Gamma^2\rangle/x$ thus determined for a-PS in cyclohexane at 34.5 °C and in CCl_4 at 25 °C are given in the fifth columns of Tables VI and VII, respectively. The value of $\langle\Gamma^2\rangle$ for cumene (x = 1) in CCl_4 is in good agreement with the value 20.8 Å^6 obtained by Suter and Flory.[13] We note that the agreement between our value of the ratio $R_{\mathrm{Hv,col}}/R_{\mathrm{Hv,total}}$ and theirs does not necessarily lead to the agreement between the two values of $\langle\Gamma^2\rangle$ itself.

V. Discussion

Dependence of $\langle\Gamma^2\rangle/x$ on x. Figure 9 shows plots of $\langle\Gamma^2\rangle/x$ against log x. The unfilled and filled circles represent the experimental values for a-PS in cyclohexane at 34.5 °C (Θ solvent) and in CCl_4 at 25 °C (good solvent), respectively. The unfilled and filled triangles represent the data for cumene in cyclohexane at 34.5 °C and in CCl_4 at 25 °C, respectively. For a-PS in each solvent, $\langle\Gamma^2\rangle/x$ increases with increasing x for small x and levels off at $x \simeq 40$, approaching an asymptotic value.

The experimental values for CCl_4 solutions are close to those for cyclohexane solutions, although the former is slightly smaller than the latter. Thus it can be said that we successfully measured $\langle\Gamma^2\rangle$ that arises from the intrinsic molecular polarizability.

Local Polarizability Tensor. We need the values of the components of the local polarizability tensor α per unit contour length to calculate the theoretical values of $\langle\Gamma^2\rangle$ for the HW chain.[26] For this purpose, it is necessary to affix a localized coordinate system (ξ, η, ζ) to a certain rigid body part in the monomer unit of the a-PS chain corresponding to that of the HW chain.[27] We take the former

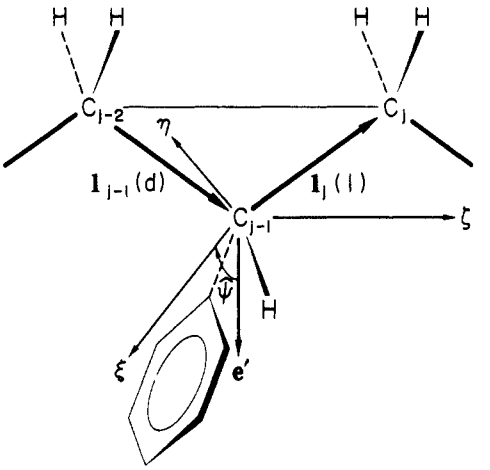

Figure 10. Rigid body part composed of the successive C_{j-2}–C_{j-1}^{α} and C_{j-1}^{α}–C_j bonds of the a-PS chain and the localized coordinate system affixed to it.

coordinate system as shown in Figure 10, where the C_{j-2}–C_{j-1}^{α} bond is d-chiral, and the C_{j-1}^{α}–C_j bond is l-chiral, according to the new Flory convention for describing stereochemical configurations of asymmetric chains.

As in ref 27, the localized coordinate system ($\mathbf{e}_{\xi_x}$, $\mathbf{e}_{\eta_x}$, $\mathbf{e}_{\zeta_x}$) affixed to the xth monomer unit consisting of the $(j-1)$th and jth skeletal bonds ($j = 2x + 4$) corresponds to the system ($\mathbf{e}_\xi$, $\mathbf{e}_\eta$, $\mathbf{e}_\zeta$) affixed to the HW chain as follows: $\mathbf{e}_{\zeta_x}$ is parallel to $\mathbf{l}_{j+1} + \mathbf{l}_j$ with $\mathbf{l}_j$ the jth bond vector, and $\mathbf{e}_{\xi_x}$ is defined by rotation of $\mathbf{e}'$ through an angle $\hat{\psi}$ about the ζ_x axis, where $\mathbf{e}'$ is a unit vector in the plane of $\mathbf{l}_{j-1}$ and $\mathbf{l}_j$ with $\mathbf{e}'\cdot\mathbf{e}_{\zeta_x} = 0$, its positive direction being chosen at an acute angle with $\mathbf{l}_{j-1}$. The angle $\hat{\psi}$ is a parameter to be determined by a comparison of the HW chain with the RIS model (or the real chain). In ref 27, the value of $\hat{\psi}$ has been determined to be $3\pi/2$ for the isotactic PS (i-PS) chain and 0 for the syndiotactic PS (s-PS) chain, from an analysis of the RIS data for the real part of the angular correlation functions $g_l^{jj'}$ of rank 1.

If we assume the additivity of the bond and group polarizabilities, the polarizability tensor β of the monomer unit becomes a sum of the contribution from the central part (C–C$^{\alpha}$HPh–C) and one-half of the contribution from the CH_2 groups on both sides. The tensor β depends on the bond rotation angles $\hat{\varphi}_{j-1}$ and $\hat{\varphi}_j$ (and also on $\hat{\psi}$). Thus we define a polarizability tensor α_0 (of the monomer unit) as the β averaged over $\hat{\varphi}_{j-1}$ and $\hat{\varphi}_j$ and relate it to the polarizability tensor α per unit contour length of the HW chain as

$$\alpha = (M_L/M_0)\alpha_0 \tag{8}$$

where M_0 is the molecular weight of the monomer unit.

In order to take the average above, we assume that the pair $(\hat{\varphi}_{j-1}, \hat{\varphi}_j)$ takes only the values at the preferred conformations: $(\hat{\varphi}_{j-1}, \hat{\varphi}_j)$ = (110°, 10°) in the gt state or (10°, 110°) in the tg state for the i-PS chain and $(\hat{\varphi}_{j-1}, \hat{\varphi}_j)$ = (10°, 10°) in the tt state for the s-PS chain.

Thus, if the bond chiralities are given as in Figure 10, the tensors α_0 for the i- and s-PS chains are given by

$$\alpha_{0,\mathrm{i\text{-}PS}} = \begin{pmatrix} 2.02 & -1.41 & 0 \\ -1.41 & 2.17 & 0 \\ 0 & 0 & -1.66 \end{pmatrix} \text{Å}^3 \tag{9}$$

and

$$\alpha_{0,\mathrm{s\text{-}PS}} = \begin{pmatrix} 2.15 & 1.46 & 0 \\ 1.46 & 2.10 & 0 \\ 0 & 0 & -1.72 \end{pmatrix} \text{Å}^3 \tag{10}$$

respectively, where the values adopted in section II have been used for the bond and group polarizability tensors. We note that when the bond chiralities are reversed, the $\xi\eta$ and $\eta\xi$ components of α_0 change sign, the other seven components remaining unchanged. Thus we regard the a-PS chain as a kind of random copolymer of i- and s-PS and assume that α_0 is given by

$$\alpha_0 = (1 - f_r)\alpha_{0,i\text{-PS}} + f_r\alpha_{0,s\text{-PS}} \quad (11)$$

where we replace the off-diagonal components of the tensors $\alpha_{0,i\text{-PS}}$ and $\alpha_{0,s\text{-PS}}$ by their absolute values.

Analysis of the Mean-Square Optical Anisotropy $\langle\Gamma^2\rangle$. The mean-square optical anisotropy $\langle\Gamma^2\rangle$ of the HW chain of total contour length L ($=M_0x/M_L$) (in the case of Poisson's ratio $\sigma = 0$) is given by eq 65 with eq 49, 67, 68, 69, and 70 of ref 26 and may be written in the form

$$\langle\Gamma^2\rangle = \lambda^{-1}L\sum_{j=0}^{2} C_j(\alpha, \kappa_0/\nu, \tau_0/\nu)f_j(\lambda L, \lambda^{-1}\nu) \quad (12)$$

where ν, C_j, and f_j are given by

$$\nu = (\kappa_0^2 + \tau_0^2)^{1/2} \quad (13)$$

$$C_0(\alpha, x, y) = \tfrac{1}{2}[2\alpha_{\zeta\zeta} - \alpha_{\xi\xi} - \alpha_{\eta\eta} - 3x^2(\alpha_{\zeta\zeta} - \alpha_{\eta\eta}) + 6xy\alpha_{\eta\zeta}]^2$$

$$C_1(\alpha, x, y) = 6[xy(\alpha_{\eta\eta} - \alpha_{\zeta\zeta}) + (2y^2 - 1)\alpha_{\eta\zeta}]^2 + 6(x\alpha_{\xi\eta} + y\alpha_{\zeta\xi})^2 \quad (14)$$

$$C_2(\alpha, x, y) = \tfrac{3}{2}(\alpha_{\xi\xi} - y^2\alpha_{\eta\eta} - x^2\alpha_{\zeta\zeta} + 2xy\alpha_{\eta\zeta})^2 + 6(y\alpha_{\xi\eta} + x\alpha_{\zeta\xi})^2$$

$$f_j(x, y) = (j^2y^2 + 36)^{-2}\{6(j^2y^2 + 36) + (j^2y^2 - 36)x^{-1} + x^{-1}e^{-6x}[(36 - j^2y^2)\cos(jxy) - 12jy\sin(jxy)]\} \quad (15)$$

with α_{ij} ($i, j = \xi, \eta, \zeta$) being the ij component of the tensor α. It is convenient for the analysis of the experimental data to use the tensor α_0 instead of α. We then have from eq 8 and 12

$$\langle\Gamma^2\rangle/x = (\lambda^{-1}M_L/M_0)\sum_{j=0}^{2} C_j(\alpha_0, \kappa_0/\nu, \tau_0/\nu)f_j(\lambda L, \lambda^{-1}\nu) \quad (16)$$

The reduced contour length λL on the right-hand side of eq 16 is related to x by the equation

$$\log x = \log(\lambda L) + \log(\lambda^{-1}M_L/M_0) \quad (17)$$

Thus the quantity $\lambda^{-1}M_L$ may be determined by fitting the theoretical $\langle\Gamma^2\rangle/x$ versus $\log(\lambda L)$ curve computed with optimal $\lambda^{-1}\kappa_0$ and $\lambda^{-1}\tau_0$ to the observed data for $\langle\Gamma^2\rangle/x$ as a function of $\log x$.

The solid curve in Figure 9 represents the values calculated from eq 14–17 with $\lambda^{-1}\kappa_0 = 3.0$, $\lambda^{-1}\tau_0 = 6.0$, and $\lambda^{-1}M_L = 843$. Here, the curve fitting has been applied to the data for the samples of $x_w \geq 5$ in cyclohexane and the data for cumene and the samples OS3 and OS4 have not been taken into account, since the end effect becomes appreciable as x is decreased (see Figure 3). The curve-fitting method allows some uncertainty in the evaluation of the above three parameter combinations. The values of $\lambda^{-1}\kappa_0$, $\lambda^{-1}\tau_0$, and $\lambda^{-1}M_L$ have been estimated to within ±1, ±1, and ±80, respectively.

Using the value of 11.1 for the characteristic ratio C_∞ evaluated from the value $\lim_{M\to\infty}\langle S^2\rangle_0/M = 8.3 \times 10^{-18}$ cm^2 determined for the a-PS by Miyaki et al.,[28] we have obtained $M_L/\lambda^{-1} = 1.63$ Å^{-2}. From the values of $\lambda^{-1}M_L$ and M_L/λ^{-1}, λ^{-1} and M_L are separately evaluated to be 22.7 ± 2.0 Å and 37.1 ± 1.0 Å^{-1}, respectively. In Table VIII are given the values of the HW model parameters for a-PS thus determined, together with those for i-PS and s-PS obtained from an analysis of the RIS data,[4,27,29] for comparison. The parameters $\lambda^{-1}\kappa_0$ and $\lambda^{-1}\tau_0$ for a-PS assume the values between those for i- and s-PS. The value of λ^{-1} for a-PS is smaller than those for i- and s-PS. Recall that in general, λ^{-1} is larger than the Kuhn statistical segment length, which is always twice the persistence length.[4] The value of M_L for a-PS is close to those for i- and s-PS, and also to the value of 40.8 Å for the PS chain fully extended to the all-trans conformation. We note that the above comparison is only temporary, since the parameters for i- and s-PS have not been determined from experimental data.

Table VIII
Values of the HW Model Parameters for Polystyrene

tacticity	f_r	$\lambda^{-1}\kappa_0$	$\lambda^{-1}\tau_0$	λ^{-1}, Å	M_L, Å^{-1}
atactic	0.59	3.0	6.0	22.7	37.1
isotactic	0	11	15	26.4	41.2
syndiotactic	1	0.8	2.3	37.5	41.9

The model parameters determined above provide information about the local conformation of a-PS. The radius ρ and pitch h of the characteristic regular helix, which the HW chain takes at the minimum zero of the total elastic potential energy, are related to κ_0 and τ_0 as $\rho = \kappa_0/(\kappa_0^2 + \tau_0^2)$ and $h = 2\pi\tau_0/(\kappa_0^2 + \tau_0^2)$, respectively. The values of ρ and h are evaluated to be 1.5 and 19 Å, respectively, for a-PS. From these values, it is found that the characteristic helix of a-PS has smaller ρ and larger h than that of, for example, atactic poly(methyl methacrylate) (a-PMMA), for which the values of κ_0 and τ_0 were determined from intrinsic viscosities $[\eta]$.[9] It is evident that such a regular helical form does not remain but is disordered completely or incompletely in solution. The static stiffness parameter λ^{-1} gives an extent to which the helical form is locally or globally preserved. Thus the characteristic helix of a-PS is preserved to a less extent than that of a-PMMA with $\lambda^{-1} = 40.5$ Å.[9]

The dashed curve in Figure 9 connects the RIS values for $f_r = 0.59$. It is seen that although the RIS values are in good agreement with the experimental data for small x, they tend to approach an asymptotic value somewhat larger than the observed values as x is increased. The agreement between the RIS values and the experimental data for small x is rather natural, since the bond polarizabilities given by eq 2 and 3 were determined so that the RIS value reproduces the experimental value for cumene in CCl_4.

In this study, we have shown that the theoretical calculations based on the HW model well reproduce the experimental data for $\langle\Gamma^2\rangle$ for a-PS with $f_r = 0.59$ if the values of the model parameters and the polarizability tensor are properly taken. We will extend the study to $\langle S^2\rangle$, intrinsic viscosity $[\eta]$, and so on for the same a-PS samples and examine whether or not the HW model can give a consistent explanation of all these properties.

Acknowledgment. We thank Professor T. Higashimura and Dr. M. Sawamoto of our Department for GPC measurements to determine the ratios M_w/M_n listed in Table III and Dr. Y. Einaga of our laboratory for valuable discussions.

Appendix. Statistical Weight Matrices

For the type-c a-PS chain with the degree of polymerization x, the statistical weight matrix $\mathbf{U}_j^{(x)}$ for the pair of

bonds $(j-1, j)$ may be written as follows: For $x \geq 3$

$$\mathbf{U}_2^{(x)} = \begin{pmatrix} 1 & \sigma' & \sigma' \\ 1 & \sigma' & \sigma' \\ 1 & \sigma' & \sigma' \end{pmatrix}, \quad \mathbf{U}_3^{(x)} = \begin{pmatrix} 1 & \sigma' & \sigma' \\ 1 & \sigma'\omega_{MM}^{(M)} & \sigma' \\ 1 & \sigma' & \sigma'\omega_{MM}^{(M)} \end{pmatrix},$$

$$\mathbf{U}_4^{(x)} = \begin{pmatrix} 1 & \sigma' & \sigma' \\ 1 & \sigma'\omega_{M\alpha} & \sigma' \\ 1 & \sigma' & \sigma'\omega_{M\alpha} \end{pmatrix}, \quad \mathbf{U}_5^{(x)} = \begin{pmatrix} \eta & 1 \\ \eta & \bar{\omega}_{MM} \\ \eta\omega' & 1 \end{pmatrix},$$

$$\mathbf{U}_6^{(x)} = \begin{pmatrix} \eta & 1 \\ \eta & \omega_{M\alpha} \end{pmatrix},$$

$$\mathbf{U}_{2j}^{(x)} = \mathbf{U}' = \begin{pmatrix} \eta & 1 \\ \eta & \omega_{\alpha\alpha} \end{pmatrix} \quad (4 \leq j \leq x),$$

$$\mathbf{U}_{2j+1}^{(x)} = \mathbf{U}''_m = \begin{pmatrix} \eta\omega'' & 1 \\ \eta & \omega \end{pmatrix} \quad \text{for meso dyad}$$

$$= \mathbf{U}''_r = \begin{pmatrix} \eta & \omega' \\ \eta\omega' & 1 \end{pmatrix} \quad \text{for racemic dyad,} \quad (3 \leq j \leq x),$$

$$\mathbf{U}_{2x+2}^{(x)} = \begin{pmatrix} \eta & 1 \\ \eta & \hat{\omega}_{\alpha\alpha} \end{pmatrix}, \quad \mathbf{U}_{2x+3}^{(x)} = \begin{pmatrix} \sigma'\eta\omega'' & 1 & \sigma'\eta \\ \sigma'\eta & 1 & \sigma'\eta\omega' \end{pmatrix} \quad \text{(A1)}$$

For $x = 1$

$$\mathbf{U}_j^{(1)} = \mathbf{U}_j^{(3)} \quad \text{for } j = 2, 3$$

$$\mathbf{U}_4^{(1)} = \begin{pmatrix} 1 & \sigma' & \sigma' \\ 1 & \sigma'\hat{\omega}_{M\alpha} & \sigma' \\ 1 & \sigma' & \sigma\hat{\omega}_{M\alpha} \end{pmatrix},$$

$$\mathbf{U}_5^{(1)} = \begin{pmatrix} \sigma'\eta & 1 & \sigma'\eta \\ \sigma'\eta & 1 & \sigma'\eta\omega' \\ \sigma'\eta\omega' & 1 & \sigma'\eta \end{pmatrix} \quad \text{(A2)}$$

For $x = 2$

$$\mathbf{U}_j^{(2)} = \mathbf{U}_j^{(3)} \quad \text{for } 2 \leq j \leq 5,$$

$$\mathbf{U}_6^{(2)} = \begin{pmatrix} \eta & 1 \\ \eta & \hat{\omega}_{M\alpha} \end{pmatrix}, \quad \mathbf{U}_7^{(2)} = \mathbf{U}_9^{(3)} \quad \text{(A3)}$$

The values of the parameters σ', η, $\omega_{MM}^{(M)}$, $\omega_{MM}^{(S)}$, ω', ω'', $\omega_{M\alpha}$, $\bar{\omega}_{MM}$, $\hat{\omega}_{\alpha\alpha}$, and $\hat{\omega}_{M\alpha}$ are given in the text.

Registry No. PS, 9003-53-6.

References and Notes

(1) Yamakawa, H. *Modern Theory of Polymer Solutions*; Harper & Row: New York, 1971.
(2) Flory, P. J. *Statistical Mechanics of Chain Molecules*; Interscience: New York, 1969.
(3) Flory, P. J. *Macromolecules* **1974**, *7*, 381.
(4) Yamakawa, H. *Annu. Rev. Phys. Chem.* **1984**, *35*, 23.
(5) Yamakawa, H.; Fujii, M. *J. Chem. Phys.* **1976**, *64*, 5222.
(6) Kratky, O.; Porod, G. *Recl. Trav. Chim. Pays-Bas* **1949**, *68*, 1106.
(7) Yamakawa, H.; Shimada, J.; Nagasaka, K. *J. Chem. Phys.* **1979**, *71*, 3573.
(8) Yamakawa, H.; Shimada, J. *J. Chem. Phys.* **1985**, *83*, 2607.
(9) Yoshizaki, T.; Nitta, I.; Yamakawa, H. *Macromolecules* **1988**, *21*, 165.
(10) Bucaro, J. A.; Litovitz, T. A. *J. Chem. Phys.* **1971**, *54*, 3846.
(11) Patterson, G. D.; Flory, P. J. *J. Chem. Soc., Faraday Trans. 2* **1972**, *68*, 1098.
(12) Patterson, G. D.; Flory, P. J. *J. Chem. Soc., Faraday Trans. 2* **1972**, *68*, 1111.
(13) Suter, U. W.; Flory, P. J. *J. Chem. Soc., Faraday Trans. 2* **1977**, *73*, 1521.
(14) Saiz, E.; Suter, U. W.; Flory, P. J. *J. Chem. Soc., Faraday Trans. 2* **1977**, *73*, 1538.
(15) Carlson, C. W.; Flory, P. J. *J. Chem. Soc., Faraday Trans. 2* **1977**, *73*, 1505.
(16) Yoon, D. Y.; Sundararajan, P. R.; Flory, P. J. *Macromolecules* **1975**, *8*, 776.
(17) Yoshizaki, T.; Yamakawa, H. *Chem. Lett.* **1987**, *1987*, 2351.
(18) Tonelli, A. E.; Abe, Y.; Flory, P. J. *Macromolecules* **1970**, *3*, 303.
(19) Flory, P. J.; Sundararajan, P. R.; DeBolt, L. C. *J. Am. Chem. Soc.* **1974**, *96*, 5015.
(20) Abe, A.; Jernigan, R. L.; Flory, P. J. *J. Am. Chem. Soc.* **1966**, *88*, 631.
(21) Hermans, J. J.; Levinson, S. *J. Opt. Soc. Am.* **1951**, *41*, 460.
(22) Konishi, T.; Yoshizaki, T.; Yamakawa, H. *Polym. J.* **1988**, *20*, 175.
(23) Tonelli, A. E. *Macromolecules* **1979**, *12*, 252.
(24) Sato, H.; Tanaka, Y.; Hatada, K. *Makromol. Chem., Rapid Commun.* **1982**, *3*, 181.
(25) Ray, G. E.; Pauls, R. E.; Lewis, J. J.; Rogers, L. B. *Makromol. Chem.* **1985**, *186*, 1135.
(26) Yamakawa, H.; Fujii, M.; Shimada, J. *J. Chem. Phys.* **1979**, *71*, 1611.
(27) Yamakawa, H.; Shimada, J. *J. Chem. Phys.* **1979**, *70*, 609.
(28) Miyaki, Y.; Einaga, Y.; Fujita, H.; Fukuda, M. *Macromolecules* **1980**, *13*, 588.
(29) Fujii, M.; Nagasaka, K.; Shimada, J.; Yamakawa, H. *Macromolecules* **1983**, *16*, 1613.